Indian Journal of Fibre & Textile Research
Vol. 46, September 2021, pp. 275-286

Effect of filler loading and orientation on alkali-treated cornhusk film reinforced epoxy laminate composites

Harwinder Singh & Arobindo Chatterjee[a]

Department of Textile Technology, Dr. BR Ambedkar National Institute of Technology, Jalandhar 144 011, India

Received 3 August 2020; revised received and accepted 19 January 2021

Cornhusk film (CHF) has been used as reinforcement in epoxy matrix to develop CHF-epoxy laminate composites (CHFEC). Subsequently, the influence of CHF loading by weight (3%, 6% and 9%) as well as the angle of orientation (0^0, 45^0 and 90^0) of its ridges on the dynamic mechanical properties of the composites has been studied. Alkali-treated CHF results in better CHF/epoxy interphase and shows improvement in composite performance. Strength-to-weight ratio (SWR) of alkali-treated CHF is increased by 7.2% as compared to that of untreated one. Dynamic mechanical analysis shows best results for 6wt% CHF loaded composites with 372 MPa storage modulus as compared to that with 212 MPa for neat epoxy. The positive shift in tan δ peak of around 8.2 °C for the composites validates the effectiveness of CHF as a reinforcing agent in epoxy matrix. The maximum increase in storage modulus is found up to 75.47%, and it retains 4 times its value in rubbery zone as compared to neat epoxy. The CHF-epoxy composites retain their homogeneity, which is further improved at higher angle of orientation of CHF. The predicted viscoelastic properties of composites from the theoretical expressions are in line with the actual results. Results of statistical analysis show that CHF loading and its orientation in the laminate are significantly affecting the overall properties of the composites. The maximum moisture absorption is found ~ 1.024%, which is much lower than the permissible standards for wood-polymer composites. CHF based epoxy laminate composite structures can be used for developing partitioning panels, decking and similar applications.

Keywords: Cornhusk-epoxy laminate composite, Cole-Cole plot, Dynamic mechanical analysis

1 Introduction

In the last decade, natural fibres have become an attractive alternative as reinforcement for the fibre-reinforced composites due to their numerous advantages, like low density, good mechanical properties, etc. as compared to their synthetic counterparts[1]. There is a growing interest in using the agro-waste products, wood industry by products, forest remnants and other lignocellulose matter as reinforcing agent in composites. Utilizing such natural biomass as reinforcement in matrix composites will not only cater the industrial requirements of the future but also will benefit the environment[2].

Epoxy is widely used as a matrix because of its strong cohesion and dense molecular structure which helps in promoting reactivity and provides superior bonding strength[3]. The compatibility between hydrophilic natural fibres and hydrophobic resin is enhanced by different chemical treatments to the fibres to modify the fibre surface[4]. Most common chemical treatment for lignocellulose is alkali treatment, which reduces the content of hemicellulose, lignin and other impurities from the fibres and helps in improving its interlocking with epoxy polymer due to increased surface roughness and surface area of the fibrous matter[5]. Alkali treatment also helps to prevent the microbial degradation of the fibrous material[6].

Dynamic mechanical analysis is the most suitable and effective way to analyze the viscoelastic properties of composites[7,8]. The temperature dependent dynamic parameters provide insight into the interfacial bonding between matrix and filler as well as structure, morphology and viscoelastic behavior of composite[9,10]. Recent studies on use of various lignocellulose as reinforcement have shown positive outcomes of the dynamic mechanical performance of respective polymer composites, viz. date palm[9], bamboo[10], jute [11,12], palmyra palm leaf [13], coir/luffa[14], hemp[15], wood flour[16], sisal[17,18], banana [19], kenaf [20] and corn husk[21].

Mohamed Hamdy *et. al*.[9] reported an appreciable improvement in storage and loss moduli up to 50% filler loading for date palm fibre reinforced epoxy composite. The damping factor of the composites is reduced as compared to pure epoxy. Chee *et. al*.[10] found that the equal proportion of bamboo and kenaf

[a]Corresponding author.
E-mail: chatterjeea@nitj.ac.in

in epoxy matrix improved the dynamic mechanical properties. The storage and loss modulus in the longitudinal direction increased much more effectively with incorporation of fibre than in the transverse direction[22]. Beyond T_g, the storage modulus ($E^{'}$) of luffa/coir reinforced epoxy composites is very high as compared to neat epoxy[14]. The T_g of alkali-treated fibre composites is improved as compared to untreated one[17]. Similar work done on nano banana fibres-polyester composites, showed that the NaOH treatment improved the storage modulus of the composite at all frequencies[19]. Addition of filler in kenaf fibre/PLA composites resulted in higher $E^{'}$ and decreased tan δ values[20]. Many researchers had studied the effect of extracted fibres from corn husk on the respective matrix composite properties[2,19-30].

The research work to identify the effect of corn husk as filler, on the mechanical properties of polymer composites, is limited to few studies of particle reinforced polymer composites only. No work has been reported in which corn husk film laminated composites were produced. In this article, the use of CHF as film and the impact of angle of orientation of the ridges of the CHF and CHF loading are reported.

The objective of the current study is to explore the effect of angle of orientation of the ridges of CHF and volume fraction of alkali-treated cornhusk film as reinforcement in epoxy matrix on the dynamic mechanical properties, coefficient of effectiveness of reinforcement, homogeneity of composites and moisture absorption properties of the resultant composites.

2 Materials and Methods

2.1 Materials

Araldite epoxy resin (AW-106) and hardener (HY-953), manufactured by Huntsman India Pvt. Ltd., were used as matrix. CHF was procured locally and films having thickness in the range of 0.4-0.5 mm were used as reinforcement. NaOH pallets and acetic acid, manufactured by sd-fine Chemicals India Ltd., and Afra silicone spray, manufactured by Aerol Formulations Pvt. Ltd., were used in this work. Customized moulds of dimensions 80mm×65mm×3.5mm were prepared from Central Institute of Hand Tools, Jalandhar, India.

2.2 Alkali Treatment

CHF was treated with 20g/L NaOH at 30^0C for 30 min as per the optimized alkali treatment conditions based upon weight loss and tensile strength of CHF[23] followed by rinsing with distilled water. After treatment, the CHF was washed several times with 5% acetic acid followed by distilled water till pH 7 was achieved. After drying for 4 h at 27^0C, samples were oven dried for an hour at 80^0C.

2.3 Fabrication of Composites

Hand layup technique was used to fabricate the laminate composites. Silicone spray was applied on the surface of the mould and cover plate to facilitate easy release of the composites. Resin and hardener ware mixed thoroughly by constant stirring and poured into the mould to form an initial layer on which alkali-treated CHF was placed avoiding formation of any air gap between the two, which is subsequently fully covered by pouring second layer of epoxy matrix on to the top of CHF. The mould was covered by top plate and excess epoxy was removed by applying weight over it. The mould is kept for settling for 4 h at 27^0C, followed by curing for 4 h at 60^0C. Nine samples (with replica of 3) were prepared by varying the percentage of CHF and its orientation. The orientation of CHF refers to the direction in which ridges of CHF were aligned with respect to the longitudinal direction of the mould (Fig. 1). Three levels each of CHF loading i.e. 3%, 6% and 9 % (by weight) and orientation of ridges (0^0, 45^0 and 90^0) were used (Table 1). Composites were prepared at different CHF loadings by putting multiple layers of CHF one over the other in between the epoxy matrix by maintaining the respective weight proportion of CHF. In between two CHF layers, a layer of epoxy matrix was present, hence forming a sandwich configuration as shown in Fig. 2.

2.4 Characterization of CHF and CHFEC

The untreated as well as treated CHF samples were characterized for tensile test using Zwick-Universal Testing machine according to ASTM D-882. Scanning electron microscopy was carried out using JEOL

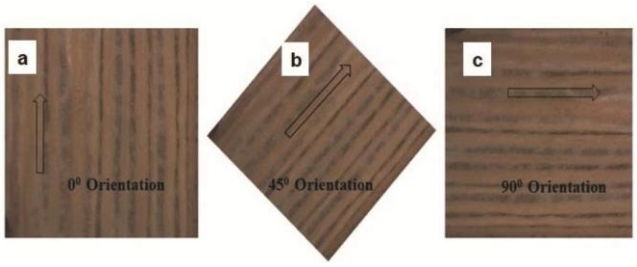

Fig. 1 — Angle of orientation of ridges of CHF with respect to longitudinal direction of the mould (a) 0^0, (b) 45^0 and (c) 90^0

Table 1 — Coded values of different CHF loadings and angle of orientation of composites

Coding	A-1-0	A-1-1	A-1-2	A-2-0	A-2-1	A-2-2	A-3-0	A-3-1	A-3-2
CHF, % (wt./wt.)	3	3	3	6	6	6	9	9	9
Orientation, deg	0	45	90	0	45	90	0	45	90

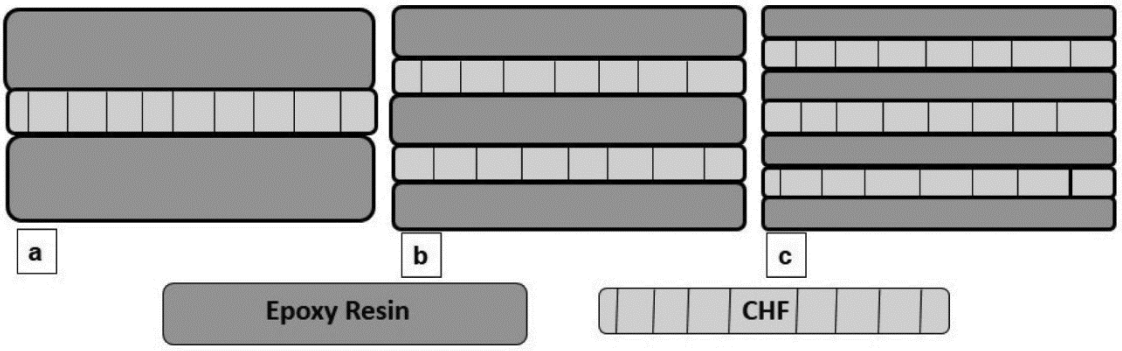

Fig. 2 — Different sandwich configuratiuons of CHFEC by varying the CHF percentage (a) 3wt%, (b) 6wt% and (c) 9wt% at 0^0 angle of orientation of ridges of CHF

(6510LV) machine at magnification levels of ×500 and ×150. Dynamic mechanical testing of the composites, having dimensions 30mm×6mm×3.2 mm, was done on DMA1 (Mettler Toledo) on single cantilever mode, at 1 Hz frequency by applying 0.1 N strain in the temperature range 27° - 140°C and ramp rate 3°C/min. Cole-Cole plots were obtained from the storage and loss moduli of the samples which show the homogeneity of the polymer system[24]. Effectiveness of the reinforcement (C) was calculated using the following formula:

$$C = (E'_g/E'_r) \text{ of Composite} / (E'_g/E'_r) \text{ of Resin}$$

where E'_g and E'_r are the storage moduli at glassy and rubbery states respectively.

2.5 Moisture Absorption Test

The moisture absorption behavior of the samples was analyzed by using ASTM-D570 standards. The specimens were cut into rectangular bars of 76.2 mm × 25.4 mm having thickness 3.2mm. The samples were conditioned at 100^0C for an hour followed by immersing in water for 24h at 27^0C. Immediately after the stipulated time, samples were taken out, wiped dry and weighed again with a precision of 0.001g.

3 Results and Discussion

3.1 Morphology of CHF and CHFEC

After alkali treatment, the surface of CHF becomes rough due to partial removal of hemicellulose and lignin. The schematic representation of effect of alkali treatment is shown in Fig. 3. The cementing walls of lignin are ruptured and surface roughness of CHF is increased, resulting in increased surface area of the CHF due to fibrillation, which consequently helps in increasing the mechanical interlocking between CHF and epoxy matrix[25,26].

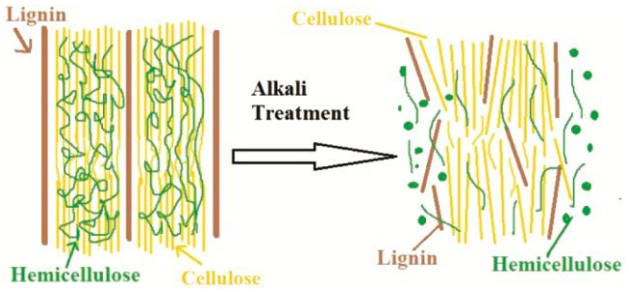

Fig. 3 — Schematic representation of the effect of alkali treatment on the structure of CHF

The SEM micrographs highlight the difference in surface morphology of the untreated and alkali-treated CHF as well as untreated and alkali-treated CHFEC (Fig. 4). The polygon type profiles on the CHF [Fig. 4(a)] are shrunk after alkali treatment [Fig. 4(b)]. The pronounced effect of delignification and partial removal of hemicellulose can be visualized from the ruptured CHF structure which results in rough topography and increased surface area[27]. Furthermore, due to shrinkage of CHF structure, 48% more number of ridges are available in an equivalent area as compared to untreated CHF, which helps in enhancing the interaction between CHF and matrix.

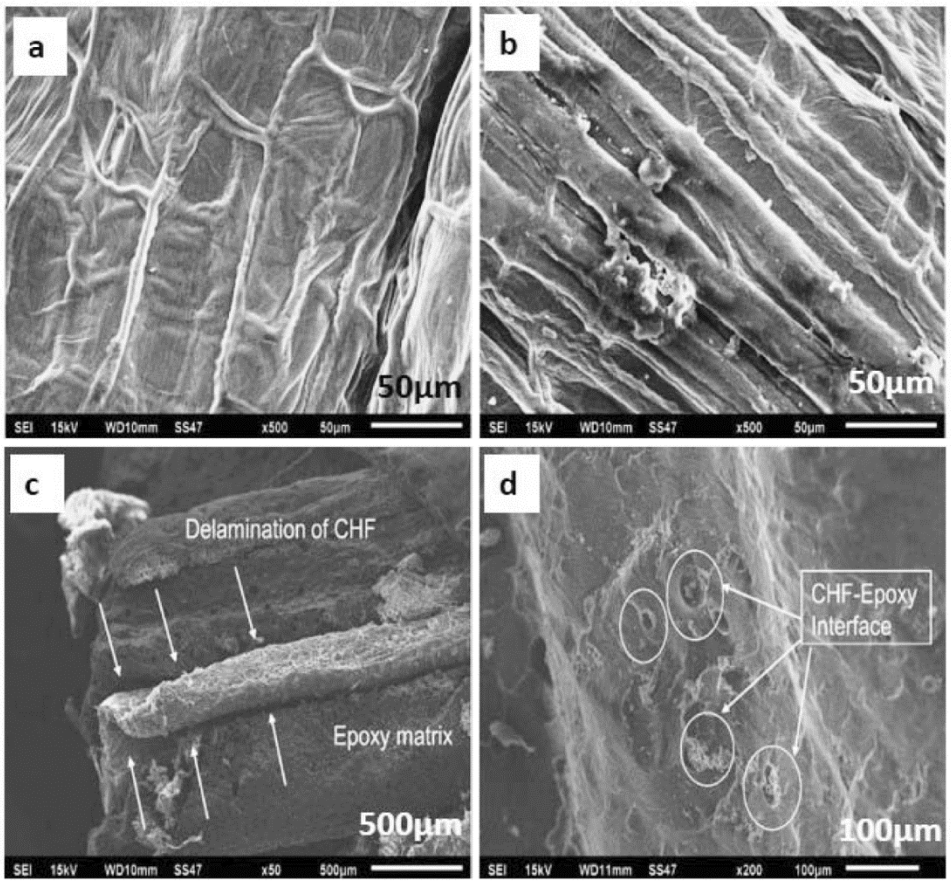

Fig. 4 — SEM images of (a) untreated CHF, (b) alkali-treated CHF, (c) untreated CHFEC and (d) alkali-treated CHFEC

Figures 4(c) and (d) show the SEM images of fractured samples of untreated and alkali-treated CHF reinforced epoxy composites. For untreated samples, interphase fails due to CHF-matrix delamination as shown in Fig. 4(c). Due to the delamination of CHF/epoxy, there is fall in the stress bearing capacity of the composite[28]. The reason for the same may be ascribed to the increased stress concentration on the matrix part as well as interfacial sliding (CHF/epoxy) friction[29], which may enhance crack propagation[30]. While the alkali-treated CHF based composite [Fig. 4(d)] shows better bonding, an improved interphase and ultimately provides better mechanical properties to the composite.

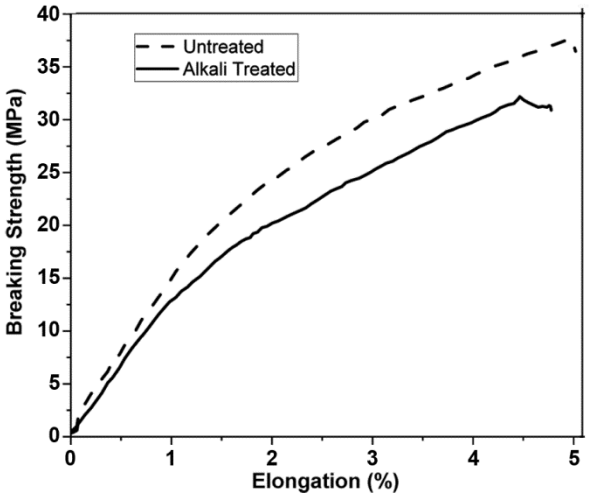

Fig. 5 — Load elongation curves of alkali-treated and untreated CHF

3.2 Tensile Properties of CHF

The alkali treatment condition of CHF are optimized based upon tensile strength and weight loss of CHF as reported earlier[23] (alkali concentration 20g/L, time 30 min and temperature 30°C). Figure 5 shows the load elongation curves of alkali-treated (optimized condition) and untreated CHF. After alkali treatment, breaking strength and elongation of CHF are found to decrease marginally (13% and 4.4% respectively). The reduction in strength is attributed to the partial disruption of the cementing walls of the CHF structure due to delignification and partial removal of hemicellulose on alkali treatment [5,27,31].

Alkali treatment of CHF also leads to loss in weight. Under optimized treatment condition, there is about 20.17% weight loss[23] . However, the strength-to-weight ratio (SWR) of alkali-treated CHF is increased by 7.2% as compared to untreated one, which is beneficial for the composites. Increase in SWR of treated CHF will have a positive influence on SWR of the composites[32].

3.3 Dynamic Mechanical Analysis

3.3.1 Storage Modulus

The storage modulus (E') vs. temperature curves of neat epoxy and alkali-treated CHFEC are shown in Fig. 6. There is increase in E' value of the composites with addition of CHF in all the cases compared to neat epoxy, though the extent of increase varies depending upon CHF% and angle of orientation of ridges of CHF. The maximum E' value is obtained for A2-1 (372 MPa), whereas the neat epoxy shows the lowest (212 MPa). The effectiveness of CHF and epoxy interphase is demonstrated by the increase in E' of composites with incorporation of CHF compared to neat epoxy. Similar trends are observed and reported by other researchers [7,18,33].

3.3.1.1 Effect of CHF Loading on Storage Moduli

Figure 6(b) shows the effect of CHF loading on storage moduli of the composites at 0° angle of orientation of CHF. The average E' of neat epoxy increases by 17% with 3wt% addition of CHF, by 55.6% at 6wt% CHF (330 MPa) and decreases slightly thereafter at 9wt% (310 MPa). The increase in E' with addition of CHF is inevitable due to restriction provided by the reinforcement to the matrix molecules[34]. The reason for slight fall in E' at 9wt% may be attributed to frictional sliding of CHF layers with increase in mobility of polymer chains of epoxy matrix[35,36]. All the composites exhibit higher E' retention in rubbery zone (50°-90°C) compared to neat epoxy. The percentage increase in retention of E' of the composites with respect to neat epoxy is maximum in case of 9wt% (429%), followed by 6wt% CHF (380%) and 3wt% CHF composite (279%) respectively. The maximum retention of E' in rubbery zone of CHFEC (49.65 MPa) for 9wt% CHF agrees well the findings of Chee et al.[10] for kenaf mat reinforced epoxy composites (48.9 MPa).

3.3.1.2 Effect of Orientation of CHF on Storage Moduli

Figure 6(c) highlights the effect of orientation of CHF on the E' of the composites at constant loading. The storage moduli of the composites are always

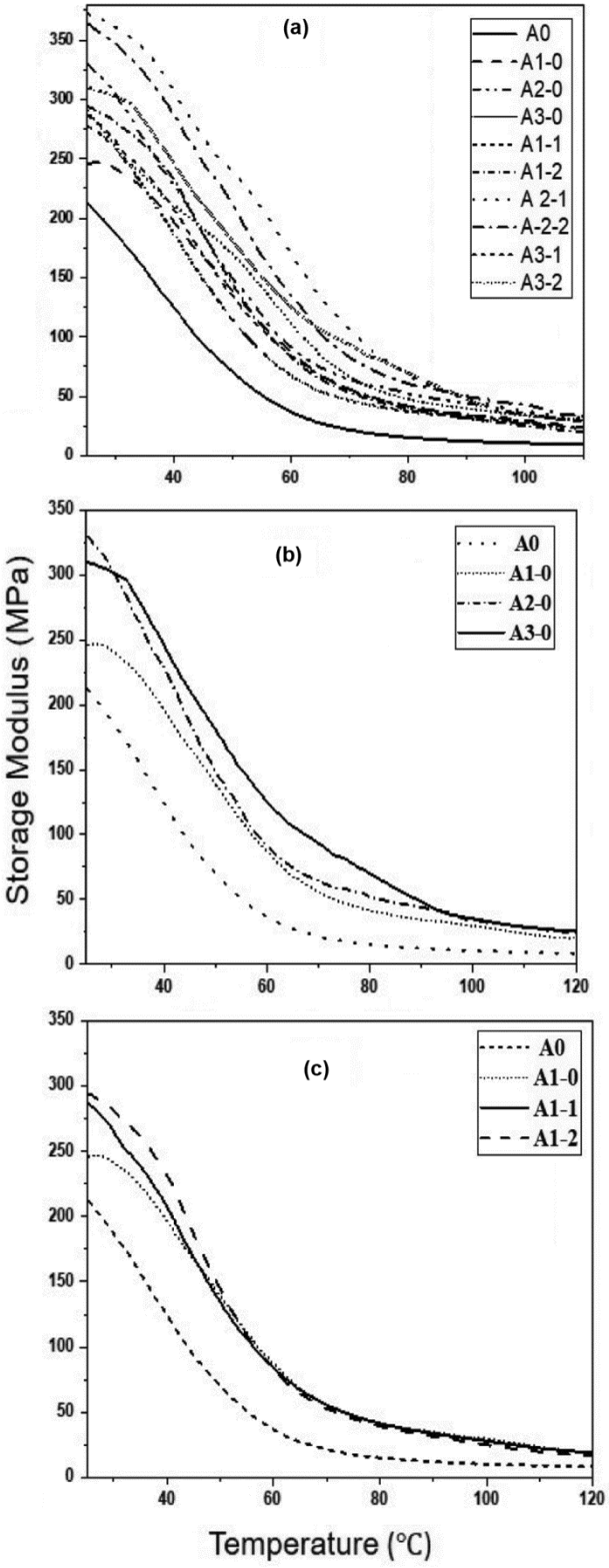

Fig. 6 — Storage moduli *vs*. temperature curves of (a) neat epoxy CHFECs, (b) at constant angle of orientation (0°) and different loadings (3wt%, 6wt% and 9wt%) and (c) at constant loading (3wt%) and varying angle of orientation (0°, 45°and 90°)

higher than that of neat epoxy throughout the temperature scan. In case of 0° angle of orientation of CHF, E' is around 246 MPa which is increased by 16% (286 MPa) and 19.5% (294 MPa) at 45° and 90° angle of orientation respectively [Fig. 6(c)]. It is observed that with increase in angle of orientation of CHF, more number of ridges are available per cm, resulting in an increased area of interface between CHF and matrix, which consequently enhances the storage moduli at higher angle of orientation of CHF. However, in rubbery zone the composites show almost similar E', may be due to increased mobility of the polymer molecules, which hinders the predominance of ridges, the other reason may be due to internal sliding of CHF layers with increase in mobility of the matrix molecules in rubbery state.

3.3.2 Loss Modulus

Figure 7 represents the loss moduli vs. temperature curves of different CHFEC and neat epoxy. E'' of the composites is increased as compared to neat epoxy for all the filler loading percentages. In case of neat epoxy, the E'' maxima is 19.34 MPa at 38.25°C which keeps on increasing with addition of CHF [Fig. 7(a)] and the highest value (40.32 MPa) is reported for 9wt% CHF loaded composites at 44.65°C. The reason for increase in E'' may be ascribed to the mechanical restrain provided by the addition of CHF to the free movement of molecular chains of the epoxy matrix[29]. As the temperature approaches rubbery state, E'' starts decreasing due to increased free movement of the polymeric chains as maximum energy is dissipated[37,38]. All CHFEC retain higher E'' in rubbery state as compared to neat epoxy. T_g obtained from both E'' and tan δ peaks for respective composites is shown in Table 2. Figure 7(b) represents the E'' values of composites at constant loading (3wt%) and varied angle of orientation. The pronounced effect of orientation of ridges of CHF is observed in glassy state due to variation in the maximum dissipation of energy from 0° to 90° angle[39]. The highest value of E'' maxima (31.72 MPa) is obtained at 42.47°C for 45° angle of CHF and it remains slightly higher throughout the test. After attaining the E'' maxima the behavior of composites is more or less similar, irrespective of orientation; this might be due to the predominance of free movement of molecular chains beyond T_g (ref. 18).

3.3.3 Tan δ

Figure 8 depicts the tan δ curves of the composites and neat epoxy. Addition of alkali-treated CHFin the composites improves the damping properties as

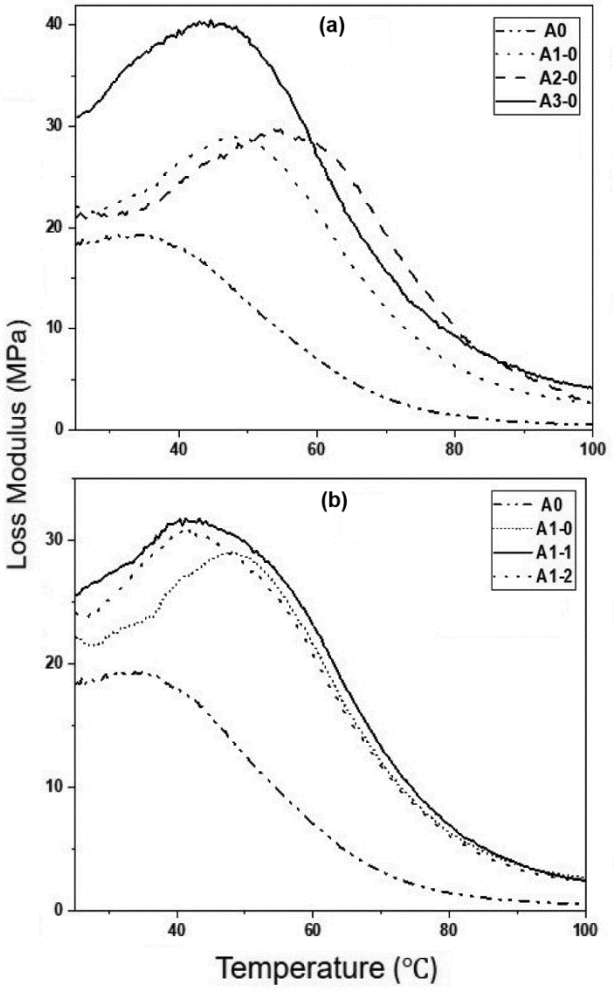

Fig. 7 — Loss moduli *vs.* temperature curves of CHFEC at (a) constant angle of orientation (0°) and different loadings (3wt%, 6wt% and 9wt%) and (b) constant loading (3wt%) and varying angle of orientation (0°, 45°and 90°)

Table 2 — Tan δ max (T_g), E'' max (T_g) and peak height of CHFEC

Composite	T_g, ^{0}C Tan δ (max)	T_g, ^{0}C E'' (max)	Damping factor (peak height)
A0	56.63	38.25	0.450
A1-0	60.90	47.81	0.251
A1-1	60.55	42.47	0.277
A1-2	61.35	43.86	0.250
A2-0	64.00	54.75	0.322
A2-1	64.35	55.62	0.354
A2-2	64.81	53.21	0.365
A3-0	56.15	44.65	0.225
A3-1	56.63	48.76	0.201
A3-2	57.85	47.81	0.234

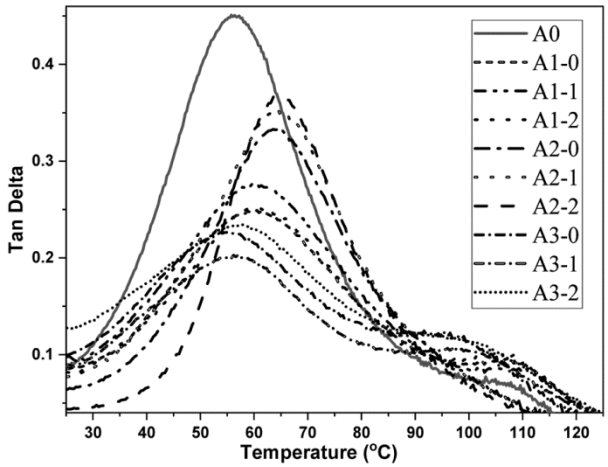

Fig. 8 — Tan δ curves of neat epoxy and CHFEC with varying CHF% and angle of orientation

compared to neat epoxy. Below T_g, all the composites show lowest values of tan δ, due to the restricted movement of polymer molecules at this stage, but as the temperature reaches T_g, molecular mobility increases, resulting in higher tan δ peak values[40,41]. The neat epoxy exhibits highest damping, while A3-1 composite shows the lowest among all (Table 2). Increasing the CHF content restrains the segmental mobility of the matrix molecules, consequently E' values of the composites are increased more as compared to E'' values, thus resulting in lower tan δ value [10]. The T_g values obtained from tan δ peaks are higher than those obtained from E'' maxima. Similar results are reported by Chee *et. al.*[10], Gupta *et. al.* [15] and Jawaid *et. al.*[38]. The positive shift in Tan δ peak for all CHFEC indicates the effectiveness of CHF as reinforcement in epoxy matrix [15]. Maximum shift in Tan δ peak is observed in case of 6wt% CHF loaded composites irrespective of orientation. The reason for smaller shift of tan δ peak in positive side in case of 9wt% CHF loaded composites as compared to 6wt% may be attributed to the internal sliding of the CHF layers at higher volume fraction because of increase in mobility of the matrix molecules. Similar values of tan δ after reinforcement are reported by Saba *et. al.* [33] and Krishna *et. al.* [42].

Apart from T_g tan δ peak is also associated to crosslinking density. Tan δ peaks are becoming broader for all CHFEC as compared to neat epoxy. A wider peak signifies delayed time for relaxation of molecules due to restricted movement of polymeric chains, emphasizing the formation of higher crosslinking density for all CHFEC, primarily as a result of improved interfacial interaction. The findings are in agreement with the results quoted by Hazarika *et. al.* [37] and Mohamed *et. al.* [43].

3.3.4 Cole-Cole Plots

Figure 9 elucidates the Cole-Cole plots of different types of the CHFECs. The semi circularity of Cole–Cole plots indicate the homogeneity of the polymeric system whereas a deviation from semi circularity indicates heterogeneity [24]. It is observed that the addition of CHF to the matrix changes the shapes of Cole–Cole plots and hence influences the dynamic behavior of the composites. All the curves of different CHFECs exhibit semi circularity with different extents of deviation/distortion. After addition of CHF the composites behave more or less like a homogeneous polymeric system [38] [Fig. 9(a)].

Figure 9(b) highlights the effect of CHF loading at constant angle of orientation (0°) of CHFEC with respect to neat epoxy. In case of 6wt% and 9wt% CHF loading, there is good semi-circular arc of Cole-Cole plots. There is improvement in the homogeneity of the composites with increase in angle of orientation of CHF (Fig. 9c) due to the increased number of ridges, which consequently enhances the effective area of interphase between CHF and matrix. The finding is consistent with observations of E' of the CHFECs as well as those reported by Laly Pothan *et. al.* [44] and Saw *et. al.* [14].

3.3.5 Effectiveness of Reinforcement

The values of coefficient of effectiveness (COE) of the composites for different CHF % and angle of orientation are given in Table 3. COE improves with increase in CHF loading from 3wt% (A1-0, 0.305) to 9wt% (A3-0, 0.275). In glassy state E' of the composites depends upon the intermolecular forces between the molecules and the packing of polymer chains while in rubbery stage E'' is governed by the effectiveness of CHF[44] consequently higher values of E' are retained (48.55 MPa) with increase in CHF loading. Angle of orientation of CHF also influences the COE. In case of 6wt% (A2-2) and 9wt% (A3-2), the COE value decreases further at 90°angle of orientation, pointing towards improved effectiveness. The reason for the improvement in COE value at 90° angle of orientation of CHF is attributed to the presence of higher number of ridges. These ridges contribute in increasing the area of interphase of CHF and epoxy matrix, resulting in better effectiveness of the former.

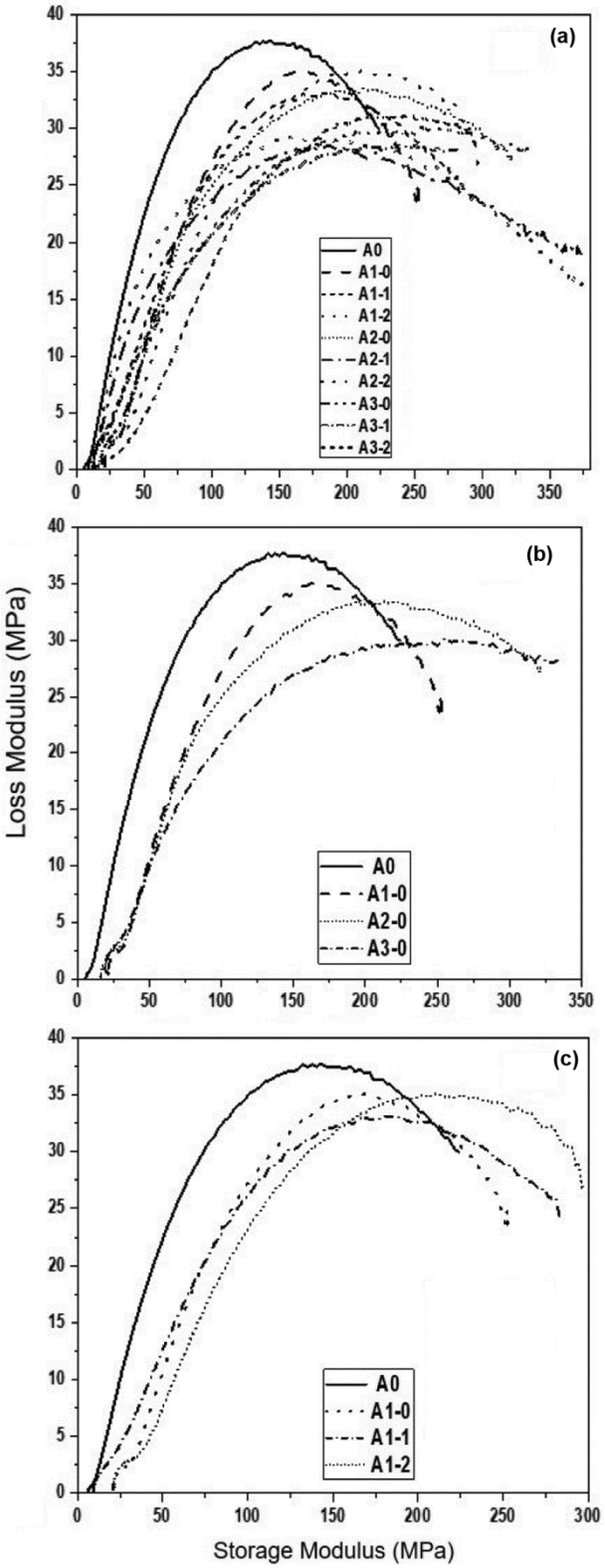

Fig. 9 — Cole-Cole plots of (a) neat epoxy and different CHFECs, (b) at constant angle of orientation (0°) and different loadings (3wt%, 6wt% and 9wt%) and (c) at constant loading (3wt%) and varying angle of orientation (0°, 45°and 90°)

Moreover, variation in COE values in case of 9wt% CHF loaded composites may be due to internal sliding of the CHF layers due to friction as the reinforcement fraction increases[30]. The COE values of the composites obtained in the current study are in line with findings from jute epoxy composites[12].

3.4 Statistical Significance of Results

The data obtained for the DMA analysis of each configuration of CHFEC is average of three readings and the summary of the statistical analysis of the experimental results is shown in Table 4. The probability of getting p-values less tha 0.05 indicates that the model terms are significant. Results of statistical analysis show that CHF loading (A) and its orientation (B) in the laminate are significantly affecting the overall properties of the composites. In case of storage modulus and Tan delta, the higher order terms of CHF are significant while for T_g both CHF and orientation significantly affect the results. The correlation factor (R Squared) and CV% values of all the response parameters are shown in Table 4. The correlation factor (R Squared) for T_g is the maximum followed by Tan δ values of the CHFEC; however, the storage modulus of the composites is having R Squared around 0.8. The reason for poor CV% in case of water absorption of the composites is due to exposure of the CHF at outer surface for 45° angle of orientation, which is discussed in detail hereunder.

Figure 10 represents the surface plots of the statistical analysis of different viscoelastic properties of the CHFEC with respect to angle of orientation (degree) and CHF loading (%). The values of storage moduli and tan δ of the composites increase with increase in CHF loading up to 6wt% and decrease thereafter [Figs 10(a) and (b) respectively). The maximum value of T_g of the composites is obtained at 6wt% CHF loading and beyond that it reduces even than that of at 3wt% CHF [Fig. 10(c)]. The COE improves with addition of CHF % and best value of COE is obtained at 9wt% CHF loading [Fig. 10(d)], which indicates the effectiveness of reinforcement.

3.5 Prediction of Viscoelastic Properties

Theoretically, the viscoelastic properties of the composites can be predicted for any volume fraction of the reinforcement based upon the experimental results obtained from the selected test conditions. The following Einstein's equations[45] are

Table 3 — Coefficient of effectiveness of CHFEC

Type	A1-0	A2-0	A3-0	A1-1	A1-2	A 2-1	A-2-2	A3-1	A3-2
$E'_{g\ Comp}$	246.12	329.79	309.94	286.76	294.23	371.90	364.04	277.84	290.05
$E'_{r\ Comp}$	34.78	44.08	48.55	34.07	31.90	46.87	49.65	31.80	39.95
COE	0.305	0.322	0.275	0.363	0.398	0.342	0.316	0.376	0.313

Table 4 — Details of ANOVA of different response parameters of CHFEC

Source	Sum of Square	df	Mean Square	F value	p-value	Status
Summary of ANOVA of storage modulus of CHFEC						
Model	10600.88	2	5300.44	11.08	0.0097	Significant
A-CHF	433.50	1	433.50	0.91	0.3778	
A^2	10167.38	1	21.26	21.26	0.0036	Significant
Residual	2869.04	6	478.17			
Cor. Total	13469.92	8				
Summary of ANOVA of Tan delta of CHFEC						
Source	Sum of Square	df	Mean Square	F value	p-value	Status
Model	0.027	2	0.013	49.80	0.0002	Significant
A-CHF	0.00232	1	0.00232	8.62	0.0261	Significant
A^2	0.024	1	0.024	90.98	0.0001	Significant
Residual	0.001615	6	0.000269			
Cor. Total	0.028	8				
Summary of ANOVA of T_g of CHFEC						
Source	Sum of Square	df	Mean Square	F value	p-value	Status
Model	82.16	3	28.72	196.93	0.0001	Significant
A-CHF	24.68	1	24.68	169.26	0.0001	Significant
B-Orientation	1.45	1	*1.45*	*9.95*	0.0253	Significant
A^2	60.02	1	60.02	411.59	0.0001	Significant
Residual	0.73	5	0.15			
Cor. Total	86.89	8				
Summary of ANOVA of water absorption of CHFEC						
Source	Sum of Square	df	Mean Square	F value	p-value	Status
Model	0.32	3	0.11	7.75	0.0251	Significant
A-CHF	0.23	1	0.23	16.27	0.0100	Significant
B-Orientation	0.00365	1	0.00365	0.26	0.6305	
B^2	0.094	1	0.094	6.72	0.0487	Significant
Residual	0.070	5	0.14			
Cor. Total	0.39	8				

Correlation factor (R Squared) and CV% values of all responses of CHFEC

Response	storage modulus	Tan δ	T_g	water absorption, %
R Squared	0.79	0.94	0.99	0.82
CV%	7.10	5.93	0.63	22.28

used for predicting the storage moduli of the composites:

$$E_c = E_m(1+ 1.25\ V_f) \quad \ldots (1)$$

$$E_c = E_m(1+ V_f) \quad \ldots (2)$$

where E_c is the storage modulus of composites; E_m , the storage modulus of matrix; V_f, the volume fraction of reinforcement. Similarly, prediction of damping behavior of the composites can be done for any volume fraction of CHF, which is a crucial factor as far as the commercial relevance of a product, is concerned. Based upon the rule of mixture for rigid reinforcements, damping factor of a composite (tan δ_c) can be predicted from the following equations by using volume fraction (V_m), and tan δ_m of epoxy matrix [44,45]. In following Eq. (4) the stiffness term (E_m / E_c) is introduced to express the minimum elastic modulus of the composites with respect to matrix in the presence of reinforcement.

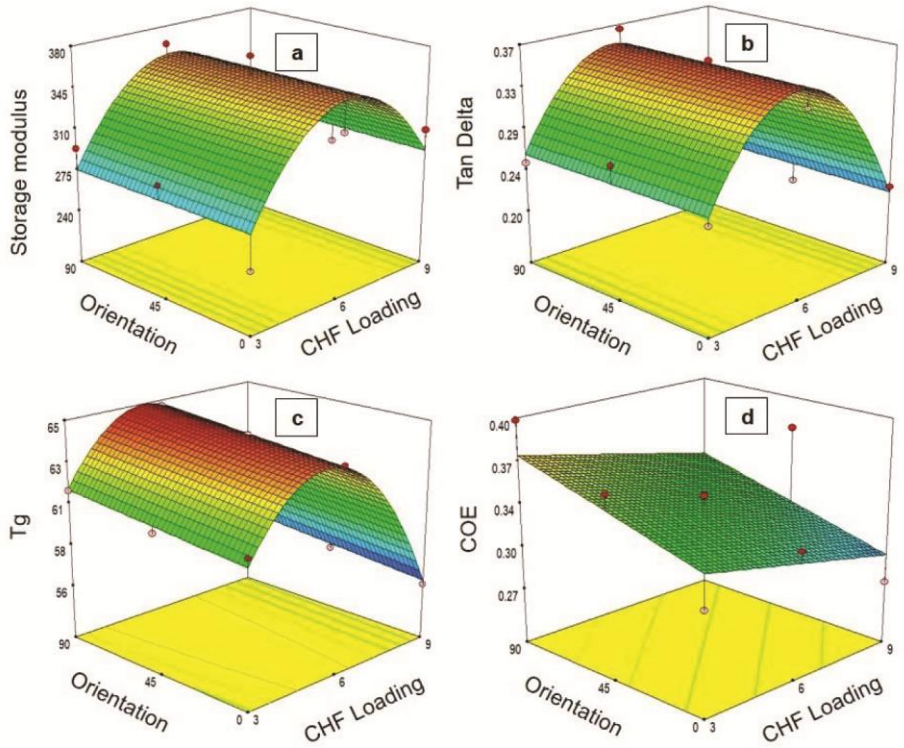

Fig. 10 — Surface plots of the CHFECs with respect to angle of orientation (degree) and CHF loading (%) (a) storage modulus (MPa), (b) Tan delta, (c) T_g (°C) and (d) coefficient of effectiveness (COE)

Table 5 — Actual and theoretical values of E_c and tan δ_c of CHFEC at different volume fractions

V_f of CHF (Loading)	E_c actual MPa	E_c (Eq.1) MPa	E_c (Eq.2) MPa	tan δ_c actual	tan δ_c (Eq.3)	tan δ_c (Eq.4)
0.163 (3%)	246.12	253.99125	245.393	0.322	0.37665	0.3229
0.326 (6%)	329.79	296.9825	279.786	0.251	0.3033	0.19405
0.489 (9%)	309.94	339.97375	314.179	0.225	0.22995	0.15654

$$\tan \delta_c = V_m \times \tan \delta_m \quad \ldots (3)$$

$$\tan \delta_c = V_m (E_m / E_c) \times \tan \delta_m \quad \ldots (4)$$

The actual and theoretical values of storage moduli (E_c) and damping factor of the composites (tan δ_c) for different volume fractions of CHF are given in Table 5. The results of storage modulus from the experimental values and that of predicted from Einstein's Eq. (1) and Eq. (2) show good relevance; however, Eq. (2) is having a better correlation with the actual results. For damping factor, Eq. (3) shows good relevance with actual results and Eq. (4) correlates well at 3wt% CHF and deviates thereafter from the experimental values. The reason for the deviation in the latter case may be attributed to frictional sliding among the CHF layers as a result of which the E_c is not achieved as per the theoretical prediction and hence tan δ_c attains higher value.

Table 6 — Moisture absorption percentage of different CHFEC

Composite	W^*_1, g	$W^{\#}_2$, g	Moisture absorption,%
A0 Neat Epoxy	8.703	8.727	0.276
A1-0 (3wt%, 0°)	8.334	8.363	0.348
A1-1 (3wt%, 45°)	8.514	8.549	0.411
A1-2 (3wt%, 90°)	8.336	8.367	0.372
A2-0 (6wt%, 0°)	8.195	8.224	0.354
A 2-1 (6wt%, 45°)	8.354	8.403	0.587
A 2-2 (6wt%, 90°)	8.281	8.314	0.399
A 3-0 (9wt%, 0°)	7.870	7.917	0.597
A 3-1 (9wt%, 45°)	8.011	8.093	1.024
A 3-2 (9wt%, 90°)	7.843	7.896	0.676

*****Initial weight.

#Weight after moisture absorption.

3.6 Moisture Absorption Properties of Composites

Moisture absorption percentage of CHFEC and neat epoxy is shown in the Table 6. It is lowest in case of neat epoxy (0.276%), which gradually increases

with increase in CHF percentage. The maximum value of moisture absorption (1.024%) is reported in 9wt% CHFEC. This increase in moisture absorption with addition of CHF can be attributed to various aspects, such as the presence of more number of hydroxyl groups with addition of CHF [46] or may be due to gaps in the CHF/epoxy interphase as the layers of CHF increases [47] or micro-cracks in the matrix [48]. It has also been observed that in all cases of 45° orientation, moisture absorption is higher irrespective of filler loading. The reason is strongly attributed to the exposure of the diagonal edges of CHF on the surface while maintaining the 45° angle during composite fabrication [49]. The moisture resistance is enhanced in case reinforcement is inside the molded surfaces as compared to the cut or exposed edges[50]. The maximum moisture absorption value of CHFEC after immersion in water for 24 h is 1.024% which is much lower than that of WPC (8.5%)[51] and permissible standards (3.00%) [46] which suggests the use of CHF composites as a substitute for the same. Furthermore, these results are statistically significant.

4 Conclusion

CHF reinforced epoxy laminate composites are successfully developed by varying the loading percentage and angle of orientation of CHF. This study demonstrates that the modification of CHF-epoxy interface by alkali treatment enhances the interfacial properties of CHFEC. It is not only due to increased surface roughness but also due to increased number of available ridges of CHF in an equivalent area as revealed from SEM images. There is marginal decrease in tensile strength of CHF after the alkali treatment, however strength to weight ratio of alkali-treated CHF is higher than untreated one. The improvement in dynamic response parameters like $3/4^{th}$ gain in storage modulus, four times more retention of E' in rubbery zone, reduced value of tan δ and positive shift of around 8° C in T_g of the composites reflect the effectiveness of CHF in the epoxy matrix. Though lowest value of coefficient of effectiveness is reported at 9wt% CHF loading, nevertheless the composites with 6wt% CHF loading showed the best values of storage modulus, loss modulus and greater shift in tan δ to the positive side. The maximum moisture absorption is around 1% for CHFEC, which is much lower than that of permissible standards (3.00%) for WPC. The DMA results of CHFEC are promising and in line with the findings reported from a number of studies based on natural fibre reinforced epoxy laminate composites. Thus, it could be envisaged that the alkali-treated CHF reinforced epoxy composites can be engineered to have end use adaptable dynamic mechanical capability. CHF can play a key role to replace the synthetic fillers for designing the lightweight laminate composites, with improved performance for various applications.

References

1 Balakrishnan P, John M J, Pothan L, Sreekala M S & Thomas S, in *Advanced Composite Materials for Aerospace Engineering* (Elsevier Ltd.), 2016, 365.
2 Reddy N & Yang Y, *Green Chem*, 7 (2005) 190.
3 Wang D, Tian B, Wangli C, Can X, Ge W & Haito C, *Polymers*, 11 (2019) 2107.
4 Muralidhar N, Kaliveeran V, Arumugam V & Srinivasula Reddy I, *J Inst Eng Ser D*, 100 (2019) 135.
5 Haghdan S & Smith G D, *J Reinf Plast Compos*, 34 (2015) 1179.
6 Jacob R & Isac J, *Indian J Pure Appl Phys*, 55 (2017) 497.
7 Idicula M, Malhotra S K, Joseph K & Thomas S, *Compos Sci Technol*, 65 (2005) 1077.
8 Saba N, Jawaid M, Alothman O Y & Paridah M T, *Constr Build Mater*, 106 (2016) 149.
9 Gheith M H, Aziz M A, Ghori W, Saba N, Asim M, Jawaid M & Alothman O Y, *J Mater Res Technol*, *8* (2019) 853.
10 Chee S S, Jawaid M, Sultan M T H, Alothman O Y & Abdullah L C, *Compos Part B Eng*, 163 (2019) 165.
11 Prasob P A & Sasikumar M, *Polym Test*, 69 (2018) 52.
12 Gupta M K & Srivastava R K, *Indian J Fibre Text Res*, 42, (2017) 64.
13 Shanmugam D & Thiruchitrambalam M, *Mater Des*, 50 (2013) 533.
14 Saw S K, in *Hybrid Polymer Composite Materials* , edited by Thakur V K, Thakur M K & Gupta R K (Elsevier Ltd.), 12 (2017) 313
15 Gupta M K, Gond R K & Bharti A, *Indian J Fibre Text Res*, 43, (2018) 313.
16 Almgren K M & Gamstedt E K, *Compos Interfaces*, 17 (2010) 845.
17 Kanny K & Mohan T P, *Compos Interfaces*, 20 (2013) 783.
18 Gupta M K & Srivastava R K, *Indian J Fibre Text Res*, 41, (2016) 235.
19 Surya Nagendra P, Prasad V V S & Ramji K, *Mater Today Proc*, 4 (2017) 9081.
20 Kwon H J, Jackapon S, Sriroth K, Park J W, Lee J H, Kim H J, Kuakoon P & Cho D, *Compos Part B Eng*, 56 (2014) 232.
21 Huda S & Yang Y, *Macromol Mater Eng*, 293 (2008) 235.
22 Karvanis K, Rusnáková S, Žaludek M & Čapka A, *IOP Conf Ser Mater Sci Eng*, (2018) 362.
23 Singh H & Chatterjee A, *Cellulose*, 27 (2020) 2555.
24 Devi LU, Bhagawan SS & Thomas S, *Polym Compos*, 2 (2009).
25 Kalia S, Kaith B & Kaur I, *Polym Eng & Sci*, 49 (2009) 1253.
26 Chirayil C J, Mathew L & Thomas S, *Reviews on Adv Mat Sci*, 27 (2014) 20.

27 Thomas M, Abraham E, Jyotishkumar P, Maria H, Pothen L & Thomas S, *Int J Biol Macromol*, 81 (2015) 768.
28 Williams KV, Vaziri R & Poursartip A, *Int J Solids Struct*, 40 (2003) 2267.
29 Gu J, Wu G & Zhang Q, *Scr Mater*, 57 (2007) 529.
30 Sreekala MS, Kumaran MG, Joseph S, Jacob M & Thomas S, *Appl Compos Mater*, 7 (2000) 295.
31 Ana Dilfi KF, Balan A, Bin H, Xian G & Thomas S, *Polym Compos*, 39 (2018) 2519.
32 Chatterjee A & Singh H, *J Inst Eng Ser D*, 100 (2019) 147.
33 Saba N, Paridah, Abdan K & Ibrahim NA, *Constr Build Mater*, 124 (2016) 133.
34 Jose C, Joy J, Mathew L, Koetz J & Thomas S, *Ind Crop Prod*, 56 (2014) 246.
35 Mallick P, in *Fibre Reinforced Composites Materials, Manufacturing, and Design*, 3rd edn (CRC Press), Chap 7, 2007, 558.
36 Gu J, Wu G & Zhang Q, *Mater Sci Eng A*, 452 (2007) 614.
37 Hazarika A, Mandal M & Maji TK, *Compos Part B Eng*, 60 (2014) 568.
38 Jawaid M, Abdul Khalil HPS, Hassan A, Dungani R & Hadiyane A, *Compos Part B Eng*, 45 (2013) 619.
39 Barkoula N M, Alcock B, Cabrera N O & Peijs T, *Poly Polym Compos*, 16 (2008) 101.
40 Safri S N A, Sultan M T H, Jawaid M & Abdul Majid M S, *Compos Struct*, 226 (2019) 111308.
41 Joseph S, Appukuttan S, Kenny J, Puglia D, Thomas S & Joseph K, *J Appl Polym Sci*, 5 (2010) 116.
42 Krishna K V & Kanny K, *Compos Part B Eng*, 104 (2016) 111.
43 Gabr M H, Elrahman M A, Okubo K & Fujii T, *Compos Part A Appl Sci Manuf*, 41 (2010) 1263.
44 Pothan L A, Oommen Z & Thomas S, *Compos Sci Technol*, 63 (2003) 283.
45 Joseph P V, Mathew G, Joseph K, Groeninckx G & Thomas S, *Compos Part A Appl Sci Manuf*, 34 (2003) 275.
46 Luo Z, Li P, Cai D, Chen Q, Quin P, Tan T & Cao H, *Ind Crops Prod*, 95 (2016) 521.
47 Adhikary K B, Pang S & Staiger M P, *Chem Eng J*, 142 (2008) 190.
48 Sari NH, Wardana ING, Irawan YS & Siswanto E, *Adv Acoust Vib*, (2016) 1 .
49 Ibrahim M I J, Sapuan S M, Zainudin E S & Zuhri M Y M, *J Mater Res Technol*, (2019) 1.
50 ASTM D570, Standard Test Method for Water Absorption of Plastics, *ASTM Stand*., 98 (2014) 25.
51 Chun KS, Fahamy N, Yang C Y, Choo H L, Pang M & Tshai K Y, *J Eng Sci Technol*, 13 (2018) 3445.